CONFIDENTIAL. Limited circulation. For review only.

Planar Surface SLAM with 3D and 2D Sensors

Alexander J. B. Trevor, John G. Rogers III, Henrik I. Christensen

***Abstract*— Semantic mapping aims to create maps that include meaningful features, both to robots and humans. We present an extension to our feature based mapping technique that allows for the use of planar surfaces such as walls, tables, counters, or other planar surfaces as landmarks in our mapper. These planar surfaces are measured both in 3D point clouds, as well as 2D laser scans. These sensing modalities compliment each other well, as they differ significantly in their measurable fields of view and maximum ranges. We present experiments to evaluate the contributions of each type of sensor.**

I. Introduction

Traditional robot maps have been used only for the purposes of localization and navigation, and have primarily focused on modeling space based on its occupancy – that is, whether or not an obstacle exists in a location or if it is free. However, as service robots become more capable and are able to perform a wider range of tasks, we believe that robot maps that provide richer information about the structure of the world are needed to help robots accomplish these tasks.

More recently, the field of *semantic mapping* has been introduced, which aims to include various types of semantic information in maps. Many semantic mapping approaches build upon traditional occupancy-grid based mapping techniques, and assign labels to individual grid-cells. Other popular approaches include appearance-based methods. Much of the work on semantic mapping has been motivated by the goals of facilitating communication with humans regarding maps, as well as enabling higher level reasoning about spaces using semantic information.

As service robots become increasingly capable and are able to perform a wider variety of tasks, we believe that new mapping systems could be developed to benefit service robots. Towards this end, we have developed a simultaneous localization and mapping (SLAM) system that uses planar surfaces as landmarks, and maps their locations and extent. We chose planar surfaces because they are prevalent in indoor environments, in the forms of walls, tables, and other surfaces.

We believe that feature-based maps are suitable for containing task-relevant information for service robots. For example, a home service robot might need to know about the locations of structures such as the kitchen table and countertops, cupboards and shelves. Structures such as walls could be used to better understand how space is structured and partitioned. Evaluation of how such maps can be used in a task relevant context is beyond the scope of this paper. We describe a SLAM system capable of creating maps of the locations and extents of planar surfaces in the environment using both 3D and 2D sensors, and present experiments analyzing the contribution of each sensing modality.

Our approach involves using multiple sensor types to measure planar landmarks. Planar surfaces can be detected in point cloud data generated by 3D sensors including tilting laser range finders, or range cameras such as the Microsoft Kinect or Asus Xtion. Range camera sensors offer extremely detailed information at close ranges, the maximum range is fairly low, and the field of view is limited. This imposes limitations on the types of environments that can be mapped using this type of sensor. In order to address these limitations, our approach also makes use of 2D laser range finders, such as those produced by SICK or Hokuyo. These sensors only provide data in a plane so they are unable to measure landmarks such as tables, shelves, or walls that do not intersect their measurement plane. However, these sensors have wide fields of view, as well as long ranges. An example of a map produced by our system is shown in Figure 1.

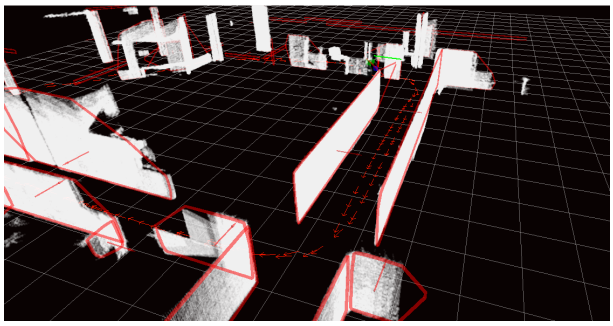

Fig. 1. An example of the type of map produced by our system. Planar features are visible by the red convex hulls, and red normal vectors. The small red arrows on the ground plane show the robot's trajectory. The point clouds used to extract these measurements are shown in white, and have been rendered in the map coordinate frame by making use of the optimized poses from which they were taken.

In Section II, we outline some key related works. We detail our mapping approach in Section III, including feature extraction for two sensor modalities, data association, and mapping. We evaluate the contributions of each measurement type in Section IV. Finally, we provide a discussion of the results and conclude in Section V.

II. Related Work

There are several areas of related work, including a wide variety of SLAM techniques, and several approaches to semantic mapping. Some of the key related works will be outlined in this section.

Since Smith and Cheeseman proposed using an EKF which was augmented with landmark positions in the state vector in [20], the Simultaneous Localization and Mapping (SLAM) problem has seen rapid development. The reference

Preprint submitted to 2012 IEEE International Conference on Robotics and Automation. Received September 16, 2011.

papers by Durrant-Whyte can be consulted for a complete review of the early years of SLAM in [6] and the current state-of-the-art in [1].

Many SLAM implementations in use today break from the traditional EKF formulation and favor graph optimization techniques. These techniques maintain the entire robot trajectory, which keeps landmarks uncorrelated and results in a very sparse representation which can be solved efficiently. Folkesson and Christensen developed GraphSLAM [8] which finds the best assignment for the robot trajectory and the landmark positions with a nonlinear optimization engine. Square Root Smoothing and Mapping (SAM) developed by Dellaert [4], exploit the sparsity of the full SLAM problem by using sparse linear algebra. By keeping the extra information of the trajectory, this technique paradoxically improves efficiency. This technique repeatedly finds the least-squares solution to a linear approximation to the measurements in the SLAM graph, rapidly converging on the solution. This technique was extended to enable incremental online operation in [9], [10]. We use the GTSAM library which Dellaert has developed as an implementation of these techniques [5].

Other techniques have focused on 3D and semantic mapping. In [18], Rusu *et.al.* found candidate objects from 3D point clouds by first segmenting horizontal surfaces and then finding clusters which are supported by these horizontal surfaces. This technique can be used to find multiple planes, and objects can be extracted which are supported by each of these planar surfaces. The plane extraction used in this work is based upon this technique [19]. These papers showed that planar surfaces can be extracted from point clouds very effectively, and objects can be found which are supported by these planar surfaces. In our approach, we use the extracted planes from point clouds as measurements of planar landmarks for larger scale scenes in our SLAM system.

Nüchter *et.al* investigated semantic labeling of points in 3D point cloud based maps in [15] and [14]. These papers demonstrated a SLAM system for building point cloud based maps based upon Iterative Closest Point (ICP)[2]. Semantic interpretation was given to the resulting maps by labeling points or extracted planes with labels such as floor, wall, ceiling, or door. This technique was applied in outdoor as well as indoor environments.

An approach to finding horizontal surfaces such as tables was investigated previously by Donsung and Nevatia [11]. The method presented in this work measured the relative pose of tables or desks with an edge-based computer vision approach. This technique was used for finding the relative pose of these surfaces from the robot's current pose, but it was not used for building large-scale maps of surfaces.

Other previous approaches to plane mapping include Pathak *et.al.* [17][16] have removed the dependency on ICP and focus on extracted planar features. ICP based techniques are susceptible to local minima particularly when there is insufficient overlap between point clouds. Extracted planar features also exhibit significant compression and computational advantages when compared to full point clouds. In [17], planar features are extracted at each robot pose. These planar features are matched against the features which were seen in prior poses to find correspondences. This technique does not make use of any odometry; therefore, the authors have developed a technique which enables them to sequentially associate planes which is more efficient than typical RANSAC techniques. The authors then compute the least squares rotation and translation which brings the associated planes into alignment. The rotation and translation are used to build an *pose graph* which is optimized. As opposed to building a pose graph, we take the alternative approach of maintaining the planar features as landmarks in the optimization problem, along with odometry.

Perhaps the most related planar SLAM approach is by Weingarten [22]. This work involves using planar features extracted from rotating laser-range finder data as features in an EKF-based SLAM framework, making use of the SPmodel. The features are represented by their normals, and bounded by an alpha shape to represent the extent of the feature, which can be extended incrementally as new portions are observed. We will use a similar feature type in our work, but with several key differences. First, we employ a graph-based approach to SLAM instead, which allows us to solve for the full robot trajectory rather than only the most recent pose. We have found this to be important for accurately mapping the extent of planes, as errors in past poses need to be accounted for and corrected in order to accurately map planar extents. Additionally, we can measure planar landmarks using multiple sensing modalities, by considering both 3D point cloud data as well as 2D laser measurements.

III. Approach

In previous work, we have demonstrated a feature-based mapping system capable of mapping features such as 2d lines. We also demonstrated how surfaces could be detected in point clouds and mapped in a global map frame, however these surfaces were not used as landmarks in this work – instead, only 2D landmarks were used, and the surfaces did not affect the trajectory, and were not updated by the SLAM optimization [21]. We now extend this to include a new feature type, 3D planar patches. A system diagram giving an overview of our system is shown in Figure 2.

A. Mapper

Our SLAM system uses the Georgia Tech Smoothing and Mapping (GTSAM) library developed by Dellaert [5]. GTSAM approaches the graph SLAM problem by using a factor graph that relates landmarks to robot poses through factors. The factors are nonlinear measurements produced by measuring various features of the types described above. The graph is optimized by converting this factor graph into a chordal Bayes Net, for which we use the elimination algorithm. To do this efficiently, it is crucial to select a good elimination ordering, which is done using the COLAMD approximate minimum degree heuristic [3]. The variables (pose and landmark features) are iteratively expressed in terms of the other variables related to them via factors, making use of the elimination order.

Preprint submitted to 2012 IEEE International Conference on Robotics and Automation. Received September 16, 2011.

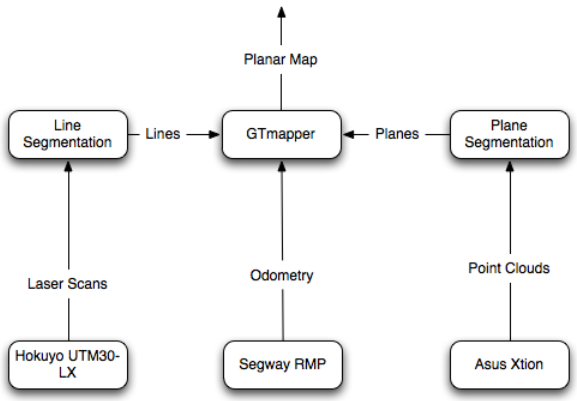

Fig. 2. A system diagram, showing an overview of our approach.

GTSAM makes it easy to add new factor types for new feature representations. The only components needed for a new factor type in the GTSAM framework are a measurement function and its derivatives. The measurement function gives the difference between the sensor measurement and the expected value computed from the relative position of the landmark from the robot.

In this work, we present a new feature type, the 3D plane. Surface normals serve as landmarks, and are optimized along with the full trajectory. Convex hulls of observed planar patches are also tracked, and hulls are required to overlap for landmarks to data associate.

B. Plane Segmentation

Our technique involves taking point cloud data of the area to be mapped. We then process these point clouds in order to segment out any horizontal surfaces such as tables that are present within each point cloud. To do this, we use the well known RANdom SAmple Consensus (RANSAC) method for model fitting [7]. In our case, we are fitting planes to the full point cloud to determine the largest plane present in each cloud.

We use an iterative RANSAC to find planes in the scene, returning the plane with the most inliers from the point cloud. We remove all inliers for this plane from our point cloud, and then perform RANSAC again to find the next largest plane. The process terminates when no plane with a sufficient number of points can be found. For each detected plane, we perform clustering on the inliers to find contiguous regions of points within our plane, discarding clusters that are too small. This clustering step serves two purposes: to remove individual points or small clusters of points that fit to the plane but aren't part of a large contiguous surface, and to separate multiple surfaces that are coplanar but are in different locations, such as two tabletops at the same height. Each cluster with a sufficient number of points is saved and will be used for mapping purposes. The resulting set of detected surface point clouds is then sent to the mapper. Point cloud data can be generated either by range camera sensors, as is used in most of this work, or by tilting laser scanners, as shown in Figure 3

For much of our point cloud processing, we use the Point Cloud Library (PCL) developed by Rusu and others at Willow Garage, which includes a variety of tools for working with 3D point cloud data including RANSAC plane fitting, outlier removal, and euclidean clustering methods. PCL is an open source library with ROS integration, and is freely available from the ROS website.

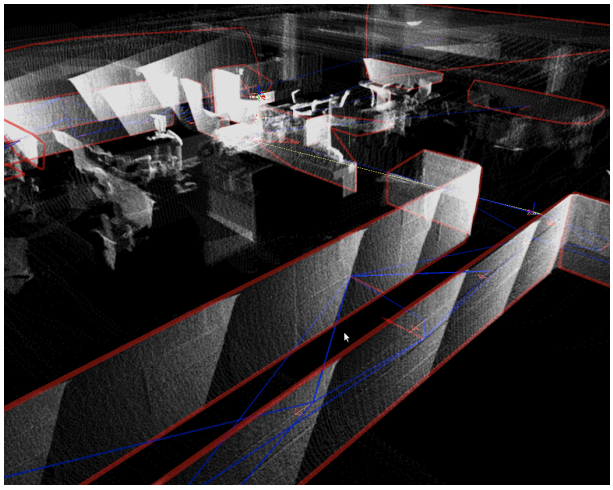

Fig. 3. An example of a map generated using a tilting 3D laser scanner to generate the point cloud data, including the full point clouds used to extract planes, as well as the planar surfaces observed. The red polygons represent the convex hulls of the mapped planes in their optimized positions.

C. Laser Line Segmentation

We use the iterative RANSAC technique to extract line segments from planar laser scanner range data from Nguyen *et.al.* [13] which is similar in principle to the method for planes described in section III-B. The laser range data is first projected into a 2D point cloud. The RANSAC iteration proceeds as follows. A pair of points is selected uniformly from the laser scan point cloud. This pair of points determines a candidate line segment. Points in the point cloud which appear within 2 cm of the candidate line segment are said to be inliers to the line segment. If the inlier set is large enough with few gaps, then this line segment is accepted and the inlier points are removed from the point cloud. A fixed number of iterations are performed to attempt to extract many of the large line segments in the range scan.

D. Plane Representation

A plane can be represented by the well known equation:

$$ax + by + cz + d = 0$$

In this work, we make use of this representation, while additionally representing the plane's extent by calculating the convex hull of the observed points. While only the plane normal and perpendicular distance are used for to correct the robot trajectory in SLAM, it is essential to keep track of the extent of planar patches, as many coplanar surfaces can exist

Preprint submitted to 2012 IEEE International Conference on Robotics and Automation. Received September 16, 2011.

in indoor environments, and we would like to represent these as distinct entities. We therefore represent planes as:

$$p = \left[n, hull\right]$$

where:

$$n = \left[a, b, c, d\right]$$

and $hull$ is a point cloud consisting of the vertices of the plane's convex hull. As planes are re-observed, their hulls are extended with the hull observed in the new measurements. That is, the measured hull is projected onto the newly optimized landmark's plane using its normal, and a new convex hull is calculated for the sum of the vertices in the landmark hull and the measurement's projected hull. In this way, the convex hull of a landmark can grow as additional portions of the plane are observed.

E. Data Association

We use a Joint Compatibility Branch and Bound (JCBB) technique for data association as in [12]. We have adapted this algorithm to work with a graph based representation instead of the EKF used in [12]. JCBB works by evaluating the joint probability over the set of interpretation trees of the measurements seen by the robot at one pose. The output of the algorithm is the most likely interpretation tree for the set of measurements. We are able to evaluate the probability of an interpretation tree quickly by marginalizing out the irrelevant portions of the graph of poses and features. The branch and bound recursion structure from the EKF formulation is used in our implementation.

F. Planar SLAM

In this section, we describe our method for mapping planes. Given a robot pose X_r, a transform from the map frame to the robot frame in the form of $(R, \vec{t})$, a previously observed feature in the map frame $(\vec{n}, d)$ and a measured plane $(\vec{n}_m, d_m)$, the measurement function h is given by:

$$h = \begin{pmatrix} R^T * \vec{n} \\ \langle \vec{n}, t \rangle + d \end{pmatrix} - \begin{pmatrix} \vec{n}_m \\ d_m \end{pmatrix}$$

The Jacobian with respect to the robot pose is then given by:

$$\frac{\delta h}{\delta X_r} = \begin{bmatrix} 0 & -n_a & n_b & \\ n_a & 0 & -n_c & [0] \\ -n_b & n_c & 0 & \\ 0 & 0 & 0 & \vec{n}^T \end{bmatrix}$$

The Jacobian with respect to the landmark is given by:

$$\frac{\delta h}{\delta n_{map}} = \begin{bmatrix} [R_r] & \vec{0} \\ \vec{X}_r^T & 1 \end{bmatrix}$$

Using this measurement function and its associated Jacobians, we can utilize planar normals and perpendicular distances as landmarks in our SLAM system. During optimization, the landmark poses and robot trajectory are optimized.

G. Laser Plane Measurements

Measurements which come from the laser line segmentation algorithm described in section III-C can be used to measure full 3D planes. This allows us to use the same formulation for measured landmarks, but with different measurement types. The laser lines measurements are under-constrained, and leave the planar landmarks with a rotational degree of freedom about the measured line, as shown in Figure 4. Landmarks that have only been measured by laser line measurements are also given a very weak prior measurement for being vertical planes, in order to constrain this degree of freedom.

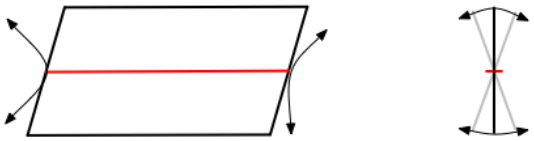

Fig. 4. A drawing demonstrating a 2D measurement of a 3D plane. Such measurements are under-constrained, and have a rotational degree of freedom about the measured line.

Line measurements on planes provide only two constraints on a mapped plane feature: a range constraint and an angular constraint. The angular constraint is that the normal to the map plane forms a right angle with a vector along the measured line. Given a robot pose X_r, a transform from the map frame to the robot frame in the form of $(R, \vec{t})$, a previously observed feature in the map frame $(\vec{n}, d)$ and a measured line with endpoints p_1 and p_2 where $\vec{b} = \frac{p_1 - p_2}{|p_1 - p_2|}$ is a unit vector along the measured line and $\bar{p} = \frac{p_1 + p_2}{2}$ is the midpoint of the line, the measurement function for laser lines h is given by:

$$h = \begin{pmatrix} \left\langle R^T * \vec{n}, \vec{b} \right\rangle \\ \langle \vec{n}, \bar{p} \rangle + d \end{pmatrix}$$

The Jacobian with respect to the robot pose is then given by:

$$\frac{\delta h}{\delta X_r} = \begin{bmatrix} \vec{p}_1 & 0 \\ \bar{p} & 1 \end{bmatrix} * \begin{bmatrix} 0 & -n_a & n_b & \\ n_a & 0 & -n_c & [0] \\ -n_b & n_c & 0 & \\ 0 & 0 & 0 & \vec{n}^T \end{bmatrix}$$

The Jacobian with respect to the landmark is given by:

$$\frac{\delta h}{\delta n_{map}} = \begin{bmatrix} \vec{p}_1 & 0 \\ \bar{p} & 1 \end{bmatrix} * \begin{bmatrix} [R_r] & 0 \\ \vec{X}_r & 1 \end{bmatrix}$$

Since an entire family of planes is consistent with a given laser line measurement, additional constraints will be required to fully constrain the graph optimization. These additional constraints can come from: another laser line measurement taken from another point of view at a different height or pitch angle, a 3D plane measurement, or a weak synthetic prior factor.

IV. Results

A. Robot Platform

The robot platform used in this work consists of a Segway RMP-200 mobile base, which has been modified to be statically stable. It is equipped with a SICK LMS-291 for obstacle avoidance and navigation, although this is not used for this work. 3D point cloud information is collected with an Asus Xtion Pro depth camera. Laser line information is collected with a Hokuyo UTM-30 laser scanner. Computation is performed on an onboard laptop; however, our experiments are run on desktop machines using log data gathered from the robot. The robot is shown in figure 5.

Although it was not used in this work, the robot is also equipped with a Schunk PG-70 gripper with custom fingers attached to a vertical linear actuator, enabling the robot to grasp objects on tabletop surfaces.

Fig. 5. The robot platform used in this work. Point cloud data is collected with the Asus Xtion Pro camera, and laser scan data is collected with the Hokuyo UTM-30. Both of these sensors are placed on the gripper near the middle of the robot. The Asus camera is mounted upside-down for more rigid and repeatable attachment.

B. Experimental Results

We collected data from office and home environments to test the performance of our SLAM system. The first two test runs were collected in the the Georgia Tech Robotics and Intelligent Machines center, and another test run was collected at a house near the Georgia Tech campus.

In the first experiment, the robot is teleoperated in the robotics student cubicle area in two large overlapping loops. The robot moves through the atrium twice in this data set. The atrium is large enough that the plane extraction filters will not find any planes close enough to the robot to make measurements during that part of the trajectory. The trajectory is relatively free of clutter so the laser line extractor has a clear view of large planar structures at all times. A photo of one of the corridors in this area is shown in Figure 8, and a floor plan is shown in Figure 12. A top-down orthographic view of the map and robot trajectory produced by our system on this dataset is shown in Figure 11.

The second experiment is a loop that passes through the hallways and a very cluttered laboratory. The hallways are narrow enough that both plane and laser measurements will be possible; however, the laboratory is both large and cluttered. The size of the laboratory will prevent finding large planar structures within the range of the depth camera so the robot not be able to make planar measurements here. The laboratory is also very cluttered, so the laser line extractor will not be able to make many long linear measurements along planar structures. A photo of the cluttered lab area is shown in Figure 9.

The final experiment is a trajectory in a house where the robot is teleoperated to examine each room. The house includes a living room, kitchen area, bedroom, hallway, and bathroom. The size of rooms and clutter of this test environment falls in between the size and clutter of the two previous test environments. The robot can be seen in this environment in Figure 5.

In order to evaluate the contributions of each sensor type, we performed a series of analyses on each data set. First, we analyzed the number of measurements of each type per pose. For all mapping runs, our robot was configured to add a pose to the trajectory on the next sensor measurement from each sensor type after traveling 0.5 meters or more according to the odometry, even if no features were detected. The results are shown in Figure 6. It can be seen that all of the datasets include several poses that have no plane measurements. This is not surprising, due to the limited field of view and range of the range camera, which was especially problematic in the open areas present in the first and second data sets, but was less of an issue in the smaller spaces of the home environment. We should also note that there were even some poses on the second dataset which also had no detected linear features, despite the wide field of view of the laser scanner. These poses occurred primarily in the lab portion of the trajectory, which includes high clutter occluding the views of the walls.

Then, in order to demonstrate that both of the sensors are contributing in different ways, we plotted the number of landmarks measured only by laser measurements, the number of landmarks measured only by 3D planar measurements, and the number of landmarks measured by both. The results are displayed in Figure 7. It is clear that both types of sensors are making contributions to the overall map, as for all datasets, there are many features measured only by the laser scanner, only by the range camera, and many features measured by both. As one would expect, there are

Preprint submitted to 2012 IEEE International Conference on Robotics and Automation. Received September 16, 2011.

more features measured only by the laser scanner in our second data set, which included larger spaces, which posed a challenge for the range camera's limited field of view and range. In general, the landmarks that were observed only by the laser scanner tended to be either out of the field of view of the range camera, or beyond its maximum range. The landmarks viewed only by the range camera often included horizontal surfaces such as tables or shelves, or planar patches that did not intersect the 2d laser scanner's measuring area. Many large planar surfaces such as nearby walls were measured by both.

Fig. 8. Another view of the Robotics & Intelligent Machines lab at the Georgia Institute of Technology, where mapping was performed.

Fig. 9. A photo of a relatively high-clutter lab in the Robotics & Intelligent Machines lab at the Georgia Institute of Technology.

V. Discussion & Conclusion

We have presented an extension to our mapping system that allows for the use of planar surfaces as landmarks. The resulting maps provide the locations and extent of surfaces such as walls, tables, and counters. These landmarks can also be measured by 2D laser range finders, and maps can be produced using both sensor modalities simultaneously.

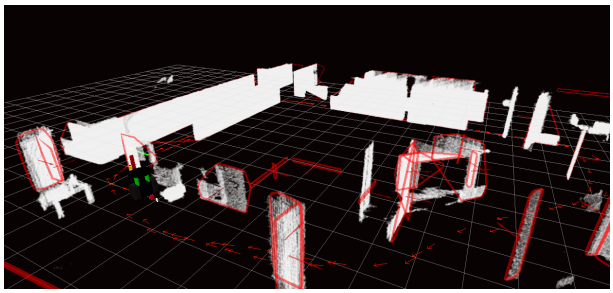

Fig. 10. A visualization of a map produced from our low-clutter office environment. Many planar features are visible, including some that have been measured only by the 2D laser scanner. Planar features are visible by the red convex hulls, and red normal vectors. The small red arrows on the ground plane show the robot's trajectory. The point clouds used to extract these measurements are shown in white, and have been rendered in the map coordinate frame by making use of the optimized poses from which they were taken.

Fig. 11. A top-down visualization of a map produced from our low-clutter office environment. Many planar features are visible, including some that have been measured only by the 2D laser scanner. Planar features are visible by the red convex hulls, and red normal vectors. The small red arrows on the ground plane show the robot's trajectory. The point clouds used to extract these measurements are shown in white, and have been rendered in the map coordinate frame by making use of the optimized poses from which they were taken.

We presented experimental results demonstrating the effectiveness of both sensor types, and demonstrated that both contribute to the mapping process.

We found that both sensor types have strengths and weaknesses. 2D laser scanners, which have long been popular for robot mapping systems, have long range and a wide field of view (40 meter range with 270 degree field of view, for our sensor), but do not produce 3D information. Landmarks that do not fall within their measurement plane cannot be observed. When mounted parallel to the groundplane, this means that important surfaces such as tables and shelves cannot be observed. Additionally, small amounts of clutter present in the plane can disrupt their ability to extract useful features.

Range cameras provide detailed information up close at a high frame rate, and allow us to map planes in any orientation, including horizontal surfaces such as tables or

Preprint submitted to 2012 IEEE International Conference on Robotics and Automation. Received September 16, 2011.

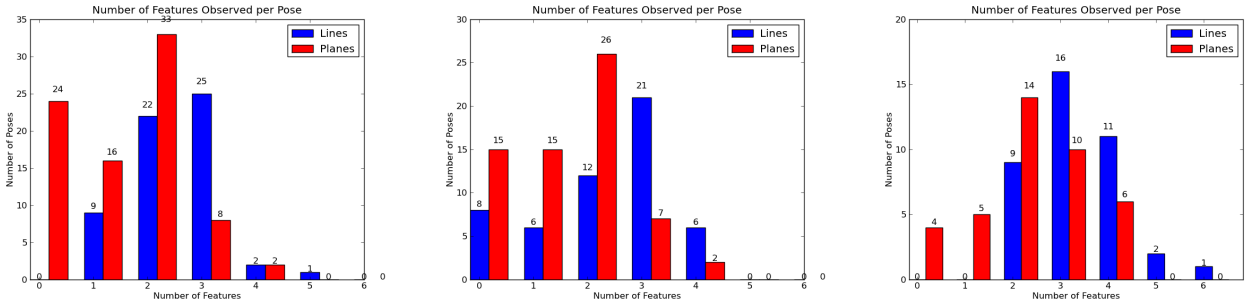

Fig. 6. Shown are the number of features observed per pose from each of our three data sets. From left to right, these include our aware. From left to right, shown are results for our low-clutter office dataset, high clutter dataset, and home environment dataset.

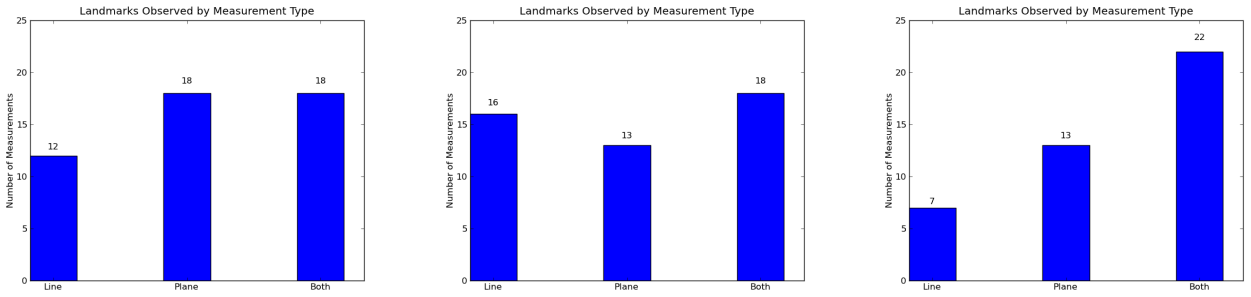

Fig. 7. Shown are the number of landmarks observed by line measurements only, plane measurements only, and measured by both. From left to right, shown are results for our low-clutter office dataset, high clutter dataset, and home environment dataset.

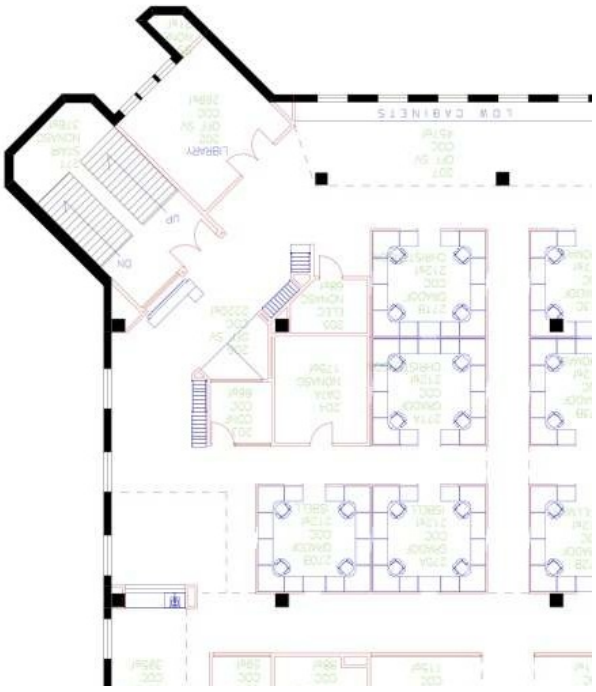

Fig. 12. A floorplan of the low-clutter area that was mapped.

desks, as shown in Figure 13. However, these sensors also have drawbacks, including a narrow field of view and and low maximum range (58 degrees horizontal, 45 degree vertical, 0.8m - 3.5m range for our sensor). These sensors were designed for gaming and user interaction rather than mapping, so while these limitations are suitable for that application as well as mapping smaller scale areas with many features, they can be problematic for mapping larger, more open spaces.

By designing a mapping system that can utilize multiple sensing modalities, we can take advantage of the strengths of each type of sensor, and ameliorate some of their weaknesses. We have found that more information can be collected by our system when using both types of sensor, which can lead to better mapping and localization performance.

VI. ACKNOWLEDGMENTS

This work was made possible through the Boeing corporation and ARL MAST CTA project 104953.

REFERENCES

[1] T. Bailey and H. Durrant-Whyte. Simultaneous localisation and mapping (SLAM): Part II state of the art. *Robotics and Automation Magazine*, September 2006.

[2] P.J. Besl and N.D. McKay. A method for registration of 3-D shapes. *IEEE Transactions on pattern analysis and machine intelligence*, pages 239–256, 1992.

[3] T.A. Davis, J.R. Gilbert, S.I. Larimore, and E.G. Ng. Algorithm 836: COLAMD, a column approximate minimum degree ordering algorithm. *ACM Transactions on Mathematical Software (TOMS)*, 2004.

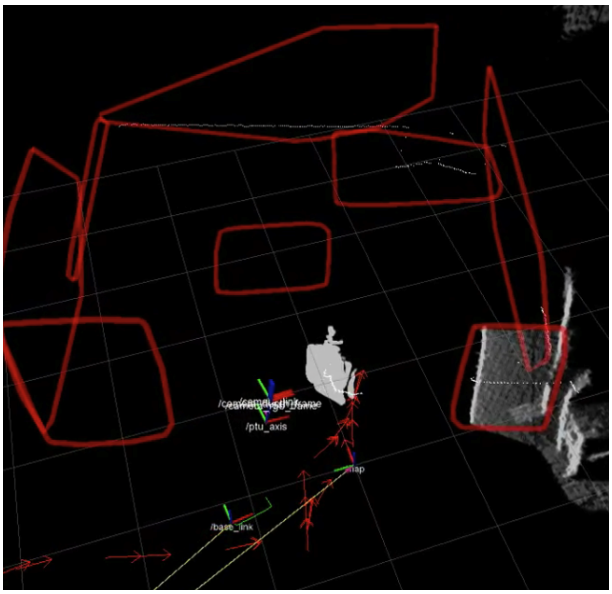

Fig. 13. A visualization of a map that includes a low coffee table, a desk, and several walls.

[4] F. Dellaert. Square root SAM: Simultaneous localization and mapping via square root information smoothing. In *Robotics: Science and Systems*, pages 24–31, Cambridge, MA, June 2005.

[5] F. Dellaert and M. Kaess. Square root SAM: Simultaneous localization and mapping via square root information smoothing. *International Journal of Robotics Research*, 25(12):1181–1204, 2006.

[6] H. Durrant-Whyte and T. Bailey. Simultaneous localisation and mapping (SLAM): Part I the essential algorithms. *Robotics and Automation Magazine*, June 2006.

[7] M.A. Fischler and R.C. Bolles. Random sample consensus: A paradigm for model fitting with applications to image analysis and automated cartography. *Comm. ACM*, 24:381–395, 1981.

[8] J. Folkesson and H. Christensen. Graphical SLAM - a self-correcting map. *International Conference on Robotics and Automation*, pages 1894–1900, April 2004.

[9] M. Kaess, A. Ranganathan, and F. Dellaert. Fast incremental square root information smoothing. In *Internation Joint Conference on Artificial Intelligence*, 2007.

[10] M. Kaess, A. Ranganathan, and F. Dellaert. iSAM: Incremental smoothing and mapping. *IEEE Transactions on Robotics*, 2008.

[11] Dongsung Kim, , and Ramakant Nevatia. A method for recognition and localization of generic objects for indoor navigation. *Image and Vision Computing*, 16:729–743, 1994.

[12] J. Neira and J. D. Tardós. Data association in stochastic mapping using the joint compatibility test. *IEEE Transactions on Robotics and Automation*, 17(6):890–897, Dec 2001.

[13] V. Nguyen, A. Martinelli, N. Tomatis, and R. Siegwart. A comparison of line extraction algorithms using 2D laser rangefinder for indoor mobile robotics. *International Conference on Intelligent Robots and Systems*, 2005.

[14] A. Nüchter and J. Hertzberg. Towards semantic maps for mobile robots. *Robotics and Autonomous Systems*, 56(11):915–926, 2008.

[15] A. Nüchter, O. Wulf, K. Lingemann, J. Hertzberg, B. Wagner, and H. Surmann. 3d mapping with semantic knowledge. *RoboCup 2005: Robot Soccer World Cup IX*, pages 335–346, 2006.

[16] K. Pathak, A. Birk, N. Vaskevicius, M. Pfingsthorn, S. Schwertfeger, and J. Poppinga. Online three-dimensional SLAM by registration of large planar surface segments and closed-form pose-graph relaxation. *Journal of Field Robotics*, 27(1):52–84, 2010.

[17] K. Pathak, N. Vaskevicius, J. Poppinga, M. Pfingsthorn, S. Schwertfeger, and A. Birk. Fast 3D mapping by matching planes extracted from range sensor point-clouds. In *Intelligent Robots and Systems, 2009. IROS 2009. IEEE/RSJ International Conference on*, pages 1150–1155. IEEE, 2009.

[18] R.B. Rusu, N. Blodow, Z.C. Marton, and M. Beetz. Close-range Scene Segmentation and Reconstruction of 3D Point Cloud Maps for Mobile Manipulation in Human Environments. In *Proceedings of the IEEE/RSJ International Conference on Intelligent Robots and Systems (IROS), St. Louis, MO, USA*, 2009.

[19] R.B. Rusu, Z.C. Marton, N. Blodow, A. Holzbach, and M. Beetz. Model-based and learned semantic object labeling in 3D point cloud maps of kitchen environments. In *Proceedings of the IEEE/RSJ International Conference on Intelligent Robots and Systems (IROS), St. Louis, MO, USA*, 2009.

[20] R. Smith and P. Cheeseman. On the representation and estimation of spatial uncertainty. *International Journal of Robotics Research*, 5(4):56–68, Winter 1987.

[21] A. J. B. Trevor, J. G. Rogers III, C. Nieto-Granda, and H.I. Christensen. Tables, counters, and shelves: Semantic mapping of surfaces in 3d. In *IROS Workshop on Semantic Mapping and Autonomous Knowledge Acquisition*, 2010.

[22] J. Weingarten and R. Siegwart. 3D SLAM using planar segments. In *Intelligent Robots and Systems, 2006 IEEE/RSJ International Conference on*, pages 3062–3067. IEEE, 2006.